

## Melting purification process and refining effect of 5083 Al–Mg alloy

Cheng-guo MA, Shu-yan QI, Shuang LI, Huan-yan XU, Xiu-lan HE

School of Materials Science and Engineering, Harbin University of Science and Technology, Harbin 150040, China

Received 28 January 2013; accepted 7 July 2013

**Abstract:** To improve the poor stability of casting process of Al alloy with high Mg content, which leads to poor final product quality, the melting purification process and the influences of the refiner on the microstructure and defect of 5083 alloy were studied. The results show that the optimized process for the rotary impeller degassing of 5083 alloy is as follows: a rotary speed of 250–400 r/min; a gas flow of 1.2–2.0 L/s, a refining time of 10–15 min. This optimized process can reduce the gas content in the solid alloy to  $2 \times 10^{-3}$  mL/g or lower. Due to the addition of grain refiner, the cast microstructure of 5083 alloy is refined. The Al–5Ti–1B wire shows the best refining effect among all the refiners. The refining effect is improved with the increase of grain refiner addition amount. And the refinement effects become stable when Ti content reaches 0.1% or higher. The surface crinkling defect of the billet can be easily found in the alloy refined with Al–5Ti–1B wire compared with the alloys refined with other refiners.

**Key words:** Al–Mg alloy; melting; purification process; grain refiner

### 1 Introduction

5xxx series aluminum alloys are widely used due to their low density, good corrosion resistance, weldability, and plasticity, as well as a moderate tensile strength [1–3]. However, a number of defects such as inclusions, coarse grain, severe surface crinkles present during the melt processing and casting of flat ingot for most of aluminum alloy enterprises. These defects induce the metallurgical defects and cracking, which decrease the quality of finished products, and slow down the popularity of the 5xxx alloy in the market [4–7].

Coarse grains are easily formed during the last crystallization stage for 5083 alloy. The coarse grains with low melting point distribute inhomogeneously among grain boundaries and dendrite boundaries, which lead to a poor performance for plasticity and tensile strength, as well as a high risk of cracking. When the grain and dendrite are refined, the low melting point phases distribute inhomogeneously among grain boundaries and dendrite boundaries, which lead to a good performance for plasticity and tensile strength, as well as a low risk of cracking [8–10]. The grain size and the state of dendrite phase are highly dependent on the quality of grain refiner.

Harmful elements and impurities in the melts are mainly eliminated by solvent purifying, online degassing and filtering. A number of techniques have been proposed in foreign countries, including the process in-furnace standing and solvent treatment,  $N_2+Cl$  treatment,  $Ar+Cl$  treatment,  $N_2+Cl+CO$  treatment, out-furnace online SNIF treatment, Alpur method, and MINT method. Purifying methods for degassing hydrogen mainly include bubbles floatation method, vacuum treatment, and ultrasonic treatment. Vacuum degassing method performs advantages over other methods, such as good eliminating performance and no pollution, while the cost is much higher than that of the others. Bubble floatation method, as a gas purifying technique, becomes more and more popular. As one of the most promising method, online degassing gains great amount of interests from aluminum melting furnace industry. Typical online degassing methods include MINT method with fixing nozzle, SNIF and Alpur method with rotary impeller.

Some critical issues for the fabrication of large-size Al alloy with high Mg ingot include poor stability of casting process, uncertainties of melt treatment and homogenization process. At present, the key techniques of melt treatment and casting for 5083 alloy are investigated to improve the quality and the yield, and

reduce the manufacturing cost [11–13].

## 2 Experimental

### 2.1 Melting process

5083 aluminum alloy used in this work was fabricated using fresh aluminum and recycled aluminum. The mass fraction of fresh and recycle aluminum was equal. The purity of fresh aluminum is 99.92%, while the recycled aluminum was composed of 99.95% Cu, 99.96% Mg and some other elements added in master alloy. Melting process was conducted in an electric furnace at the temperature of 700–750 °C. Stirring and refining were conducted for 10 min before furnace import.  $\text{JRJ}_2$  solvent protection and no stirring were required during melting process. The melt was refined with Ar for 15 min in static furnace. The melt was soaked with solvent protection for 30 min. Hydrogen content was tested after soaking for 10 min. Casting was performed when the hydrogen content was up to the standard. The casting parameters were as follows: ingot specifications of 255 mm×1500 mm, casting speed of 90–95 mm/min, casting temperature of 695–710 °C, water pressure of 0.08–0.15 MPa. 40ppi ceramic filters and ceramic filter tube were used for purifying.

The degassing and purifying parameters for 5083 melt were as follows: melt mass of 50 kg, gas type of  $\text{N}_2$  (99.9%); gas flow of 1.0, 1.2, 1.5, 2.0 L/s; rotary velocity of 100, 150, 200, 300, 450 r/min; degassing period 5, 10, 15, 20, 25 min.

### 2.2 Grain refining process

To investigate the effect of types and addition content of grain refiner on grain refinement, Al–Ti master alloy bulk, Al–Ti wires, Al–Ti–B wires and Al–Ti–C wires were selected as grain refiners. The influences of refiner type and its adding amount on grain size were studied. Casting was conducted according to the following parameters: ingot size of 255 mm×1500 mm, casting temperature of 715 °C, starting period for casting of 30 min, casting time of 102 min and cooling water pressure of 0.08 MPa. The microstructures of samples were analysed by Neophot-2 optical microscopy. The content of hydrogen in Al liquid was tested by JR-CQ apparatus.

## 3 Results and discussion

### 3.1 Effect of processing parameter on melt purification of Al alloy

Figure 1(a) shows the effect of degassing time on gas content of the melt with rotary speed of 300 r/min and gas flow of 1.5 mL/min. It indicates that as degassing time increase, the hydrogen content of alloy

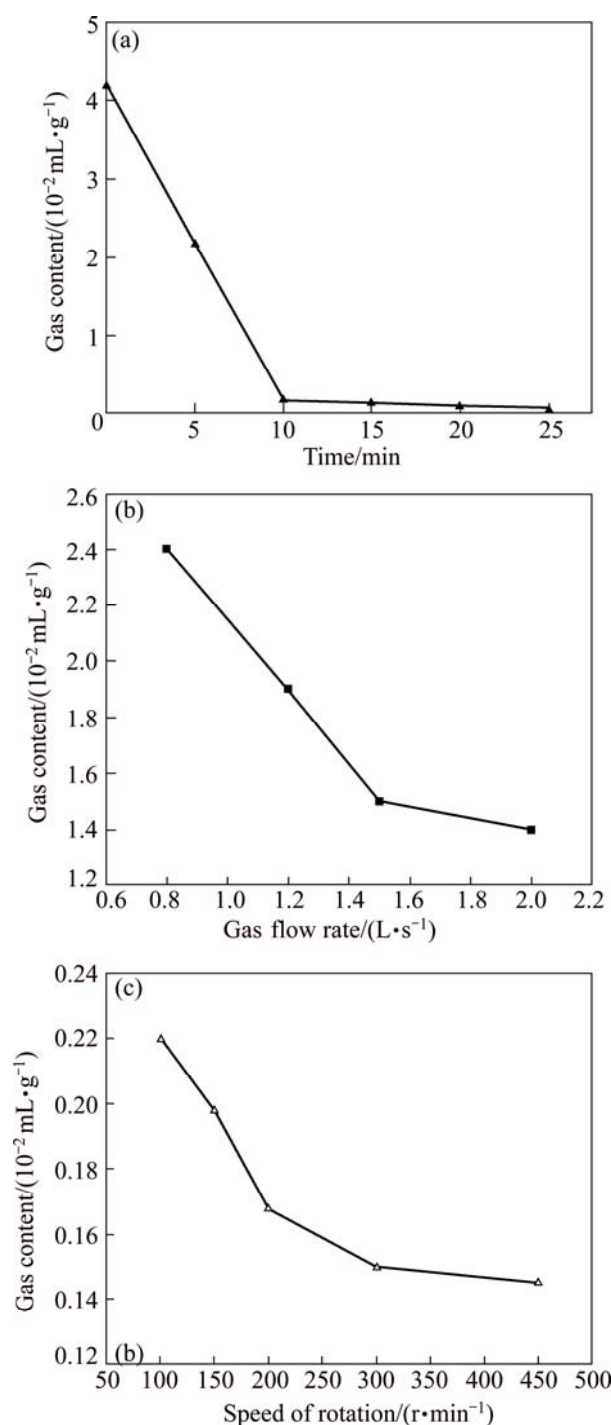


**Fig. 1** Influence of parameters on gas content: (a) Degassing period; (b) Gas flow; (c) Rotary speed

decreases significantly. The hydrogen content decreases rapidly during the first 10 min degassing period. Longer degassing period brings very little effects after 10 min. Hence actual degassing period is normally 10–15 min [14,15].

Figure 1(b) shows the influence of gas flow on degassing performance with fixed rotary speed of 300 r/min for 15 min. It indicates that the hydrogen content of alloy decreases significantly with the increase of gas flow. When the gas flow increases to 1.5 L/s, the

degassing effect is optimal, further increase of gas flow produces little degassing improvement, so the gas flow is normally set to 1.5 L/s.

As the increase of the gas flow leads to the formation of larger bubble, the increase of the rotary speed is necessary to balance the gas flow influence and decrease the gas porosity. However, it should be ensure that the rotary speed increase will not result in the writhing of the liquid surface. Gas flow and rotary speed are interrelated factors, so there is a maximum rotary speed for a given gas flow. Rotary speeds above the maximum value bring very little contribution for purifying processing. Hence, a proper rotary speed is important to improve purifying efficiency.

Figure 1(c) shows the effect of rotating speed on gas content for a fixed gas flow of 1.5 L/s and degassing time of 15 min. It shows that gas content of the melt decreases significantly with the increase of the rotating speed in the range of 100–300 r/min. Further increase of the rotary speed brings little degassing effect. Therefore, the rotary speed is normally set to 250–400 r/min.

Gas flow speed is necessary to guarantee the degassing process of molten aluminum alloy. Reaction speed is proportional to gas flow and removing efficiency of hydrogen. The larger the gas flow is, the faster the reaction is and the higher the efficiency of dehydrogen is. As gas flow rate reaches to a certain value, the ratio of interface between the liquid and the gas

decreases because of the bubble merging phenomenon. In a conclusion, the rotary injection degassing process for 5083 alloy includes rotating speed of 250–400 r/min, gas flow of 1.2–2.0 L/s and period of 10–15 min. And the gas content of solid metal can decrease to  $2 \times 10^{-3}$  mL/g or lower.

### 3.2 Effect of refiner on microstructure of 5083 alloy

Microstructures of 5083 alloy ingot are mainly  $\alpha$ (Al) phase,  $\beta$ (Mg<sub>2</sub>Al<sub>3</sub>), (FeMn)Al<sub>6</sub> and Mg<sub>2</sub>Si. Different type of grain refiner has significant influence on the microstructure. The effect of grain refiner on the microstructure of 5083 alloy is shown in Fig. 2.

It can be seen that the grain size is refined obviously after adding refiner. The coarse dendrite which is in millimeter scale in the alloy without refiner appears from the center to the edge. However, the grain size decreases significantly in the alloy with refiner. Although the grain refiner is added with the same Ti content of 0.1%, there is a significant difference in refining effect for different types of refiners. Al–5Ti–B wire and Al–5Ti wire show the best refining performance, which gains fine equiaxed grain and part of spherical grain. Comparatively, the grain size of the alloy refined with Al–3Ti–0.32C is relatively coarser and inhomogeneous. The grain size of the alloy refined with Al–5Ti bulk is much larger compared with that with Al–5Ti–B wire and Al–5Ti wire.

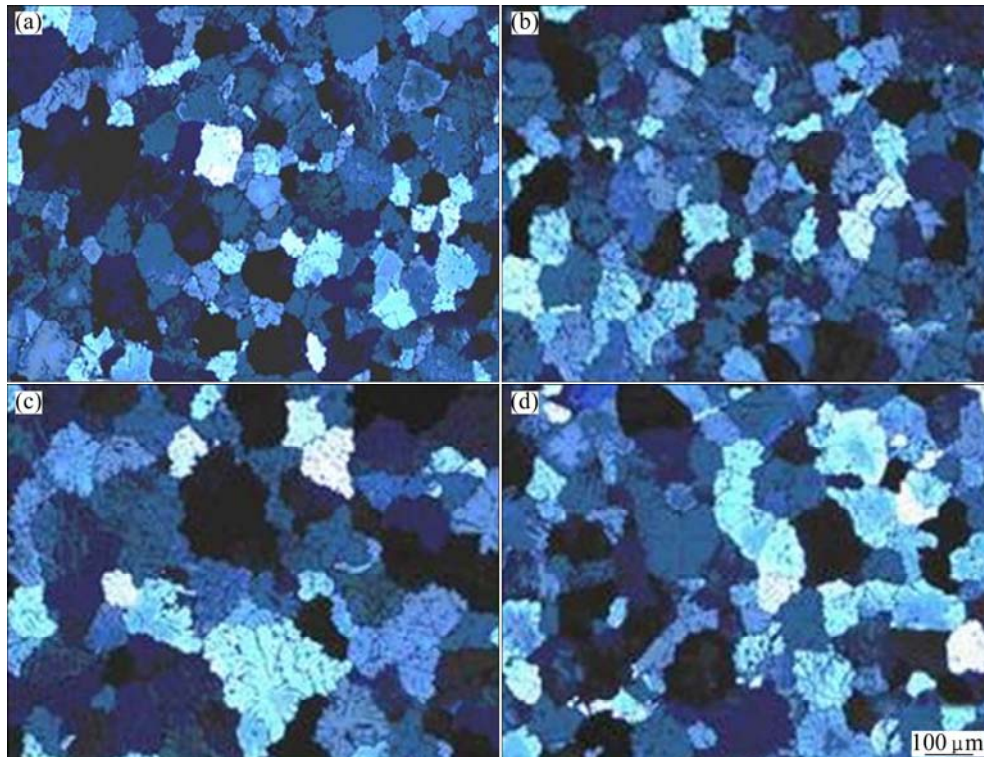


**Fig. 2** As-cast microstructures of 5083 alloy refined with different grain refiners: (a) Al–5Ti wire; (b) Al–5Ti–B wire; (c) Al–3.2Ti–0.32C wire; (d) Al–5Ti bulk

Figure 3 shows the effect of the type of grain refiner on the grain size. It indicates that the grain size is the smallest after adding Al-5Ti-B refiner, suggesting that Al-5Ti-B refiner provides the best refining effect. Therefore, the influence of the content of Al-5Ti-B refiner on the grain size is detailedly studied, as shown in Fig. 4.

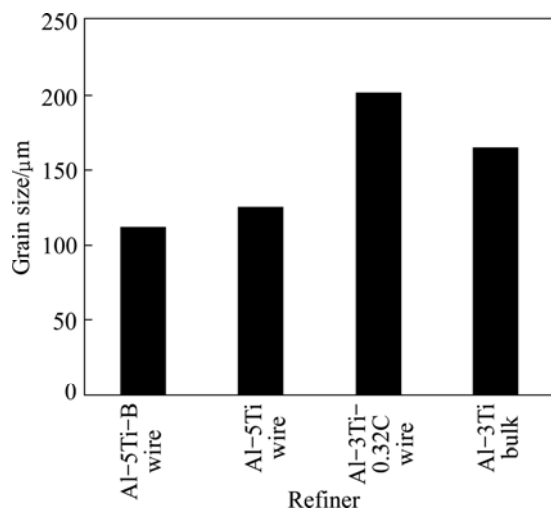


Fig. 3 Effects of type of refiner on grain size of 5083 alloy

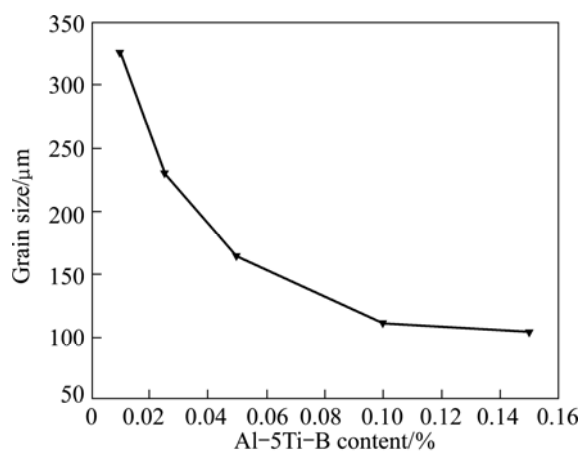


Fig. 4 Influence of amount of Al-5Ti-B refiner on grain size of 5083 alloy

The amount of the grain refiner addition greatly influences the grain size of the alloy. A small amount of 0.01%Ti can produce significant refinement. The addition of more refiner provides a further refinement for the grain size. However, when the amount of Ti in the refiner is more than 0.1%, the grain size shows no obvious change. Hence, for a given grain refiner with Ti element addition, there is an optimal adding amount. For the refining process in this work, the optimal adding amount of Ti is 0.1%.

### 3.3 Effect of refiner on surface quality of 5083 alloy

Al-5Ti-1B, Al-3Ti-0.32C and Al-5Ti wire are usually used as refiner in the production of 5083 alloys.

In these refiners, Al-5Ti-1B wire provides the best refining performance. However, the defect of surface crinkling frequently exists in the alloys refined with Al-5Ti-1B in the actual production process, which greatly decreases the quality of the ingot. It should be noted that these surface crinkling is not observed in the alloy refined with other refiners, as shown in Fig. 5.

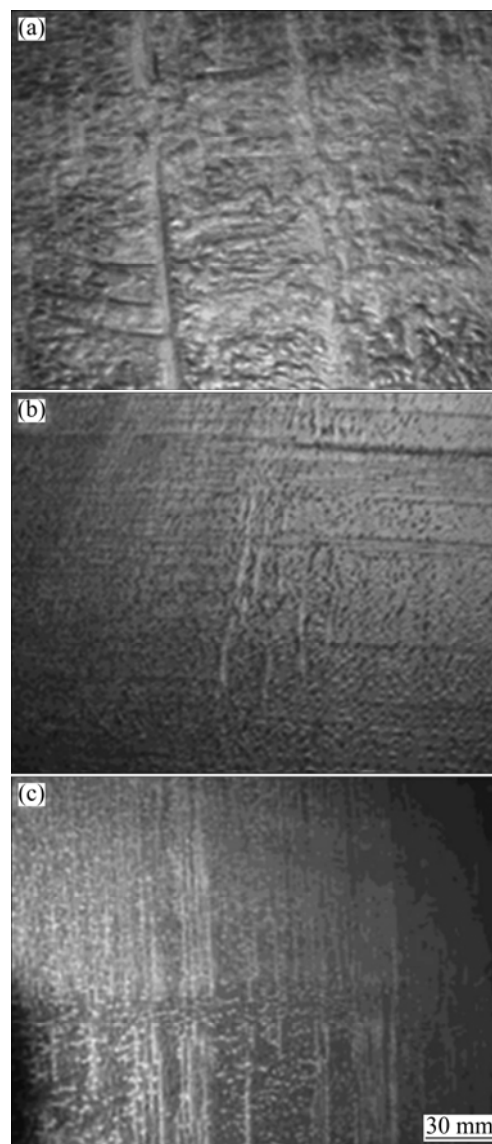
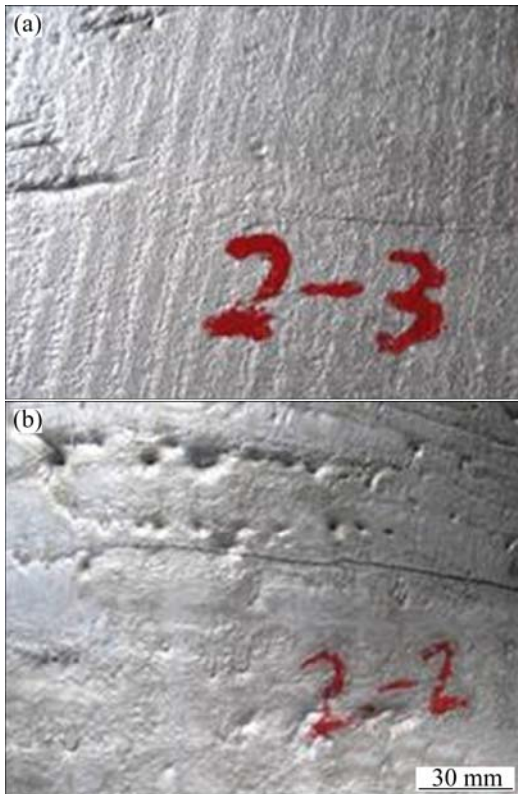


Fig. 5 Surface crinkling of ingot refined with different refiners: (a) Al-5Ti-1B wire; (b) Al-3Ti-0.32C wire; (c) Al-5Ti bulk

The surface morphology of the ingot refined by Al-5Ti-1B wire is shown in Fig. 5(a). It is found that the surface crinklings is serious, and there are many surface crinkling as long as 100 mm. The segregation tumor is also observed in the alloy refined with Al-5Ti-1B wire. Serious crinkling defects with different folding size and depth are found in a set of the trial ingots. In contrast, the alloys refined with Al-5Ti wire and Al-5Ti bulk show very slightly or no crinkling. The ingot refined by Al-3Ti-0.32C shows similar surface morphology to that

of the alloy refined with Al–Ti refiner, as shown in Fig. 5(b) and (c).

On the other hand, in the alloy refined with Al–5Ti–1B wire, macro-cracks are also observed on the surface of the ingot with surface crinkling, as shown in Fig. 6. The crack is parallel or vertical to each other. The cracks are located at both two ends of the cross section of the ingot and the congregating region of the crinkling.



**Fig. 6** Cracks on ingot surface at different locations: (a) Perpendicular to crinkling direction; (b) At end of ingot

The crack on the surface is observed after that the ingots with different refiners are rolled. The results indicate that obvious crack is found in the ingot with the crinkling. However, there are no obvious crack in rolled ingot without surface crinkling, as shown in Fig. 7.

Further analysis demonstrates that the crack source exists in the ingot with surface crinkling. The crack propagates during the deformation of the rolling process. These cracks generate after the rolling has a negative effect on 5083 alloy. According to the surface quality, the surface crinkling of 5083 ingot refined with Al–5Ti–1B is most serious. This is mainly attributed to relatively high viscosity of the melt which is partly contributed by  $TiB_2$  particle with high melting point crowded in Al–5Ti–1B. When the viscosity of the melt increases,  $TiB_2$  particles become more crowded, so they may be considered as inclusion, which will immigrate with the liquid to the surface of the ingot during the

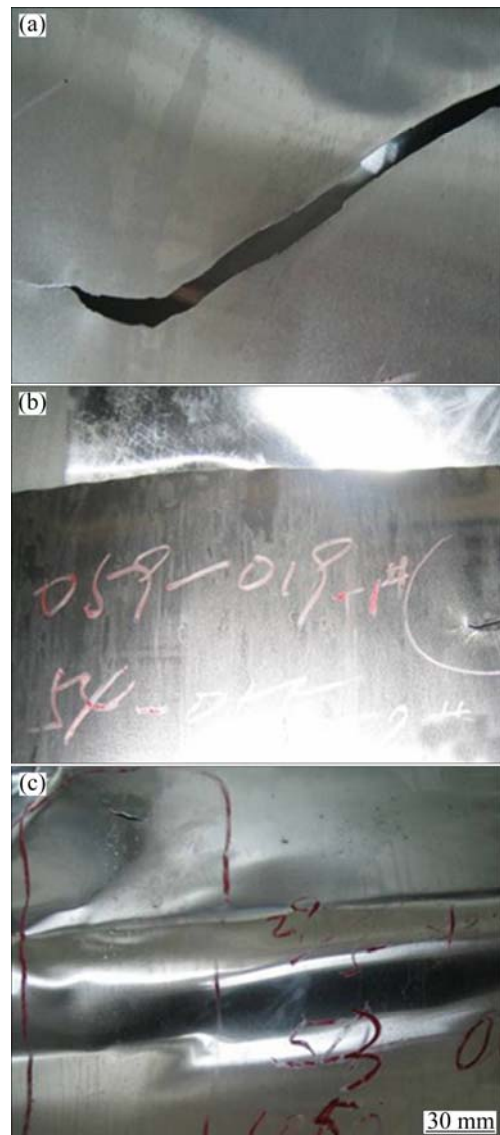


**Fig. 7** Photos of cracks after rolling of ingot refined with different refiners: (a) Al–5Ti–1B wire; (b) Al–3Ti–0.32C; (c) Al–5Ti bulk

crystallization process of the melt, leading to the uneven distribution of  $TiB_2$  particle on the surface of the ingot. This provides favorable condition for the formation of the surface crinkling defect. TiC particles in Al–3Ti–0.32C wire also possess high melting point. Although TiC particles perform similar influencing mechanism on the ingot to that of  $TiB_2$  particle in Al–5Ti–1B wire, they produce less contribution to the crinkling on the ingot surface, which may be because of dispersive distribution of TiC particles.

#### 4 Conclusions

1) The parameters of rotary impeller degassing refinement for 5083 alloy is as follows: a rotary speed of

250–400 r/min; a gas flow of 1.2–2.0 L/s, a refining period of 10–15 min. The gas content in solid phase alloy can be decreased to  $2 \times 10^{-3}$  mL/g or lower.

2) Comparatively, Al–5Ti–1B wire shows the best refining effect, and Al–5Ti is slightly inferior to Al–5Ti–1B, followed by the Al–3Ti–0.32C. Refining process of 5083 alloy improves with the increasing amount of refiner addition. When refiner contains 0.1% or higher Ti, there is very limited further refinement.

3) The defect of surface crinkling and crack frequently exist in the alloys refined with Al–5Ti–1B in the actual production process. Its main reason may be due to uneven distribution of TiB<sub>2</sub> particle on the surface of the ingot. To eliminate crinkling defect of the ingot surface, the main methods include the reducing of the B adding amount and the improvement of the temperature uniformity of ingots.

## References

- [1] LU S L, WU S S, LIN C, HU Z Q, AN P. Preparation and rheocasting of semisolid slurry of 5083 Al alloy with indirect ultrasonic vibration process [J]. *Materials Science and Engineering A*, 2011, 528(29–30): 8635–8640.
- [2] TELLKAMP V L, LAVERNIA E J. Processing and mechanical properties of nanocrystalline 5083 Al alloy [J]. *Nanostructured Materials*, 1999, 12(1): 249–252.
- [3] AHN B M, NEWBERY A P, LAVERNIA E J, NUTT S R. Effect of degassing temperature on the microstructure of a nanocrystalline Al–Mg alloy [J]. *Materials Science and Engineering A*, 2007, 463(1–2): 61–66.
- [4] AHN B M, LAVERNIA E J, NUTT S R. Dynamic observations of deformation in an ultrafine-grained Al–Mg alloy with bimodal grain structure [J]. *Journal of Materials Science*, 2008, 43(23–24): 7403–7408.
- [5] ZHANG M L, CAO P, HAN W, YAN Y D, CHEN L J. Preparation of Mg–Li–La alloys by electrolysis in molten salt[J]. *Transactions of Nonferrous Metals Society of China*, 2012, 22(1): 16–22.
- [6] WANG S R, WANG M, KANG S B, CHO J H. Microstructure comparison of ZK60 alloy under casting, twin roll casting and hot compression [J]. *Transactions of Nonferrous Metals Society of China*, 2010, 20(5): 763–768.
- [7] ZHAN M Y, ZHANG W W, ZHANG D T. Production of Mg–Al–Zn magnesium alloy sheets with ultrafine-grain microstructure by accumulative roll-bonding [J]. *Transactions of Nonferrous Metals Society of China*, 2011, 21(5): 991–997.
- [8] ZHANG H, WEI G, ZHENG L, LI L, WANG X Y, VAIDYA A. Numerical and experimental studies of substrate melting and resolidification during thermal spraying [J]. *Journal of Materials Science and Technology*, 2003, 19(S): 137–140.
- [9] ROY I, CHAUHAN M, LAVERNIA E J, MOHAMED F A. Thermal stability in bulk cryomilled ultrafine-grained 5083 Al alloy [J]. *Metallurgical and Materials Transactions A: Physical Metallurgy and Materials Science*, 2006, 37(3): 721–730.
- [10] ZHONG W M, LESPERANCE G, SUERY M. Interfacial reactions in Al–Mg (5083)/SiCp composites during fabrication and remelting [J]. *Metallurgical and Materials Transactions A: Physical Metallurgy and Materials Science*, 1995, 26(10): 2637–2649.
- [11] STANICA C, MOLDOVAN P. Aluminum melt cleanliness performance evaluation using PoDFA (porous disk filtration apparatus) technology [J]. *UPB Scientific Bulletin, Series B: Chemistry and Materials Science*, 2009, 71(4): 107–114.
- [12] SCHAEFERS W, KRUEGER J G, STEINHAEUSER T. Partial vacuum degassing—A new purification method for aluminum melts [J]. *Giesserei*, 1986, 73(14–15): 432–436.
- [13] TURCHIN A N, ESKIN D G, KATGERMAN L. Numerical evaluation of cyclone application for impurities removal from molten aluminum [J]. *Metallurgical and Materials Transactions B: Process Metallurgy and Materials Processing Science*, 2008, 39(2): 364–373.
- [14] ZENG J M, LIANG H Q, HAO C G. Flux jet technique for purification of molten aluminum [J]. *Materials Science Forum*, 2012, 704(6): 1197–1200.
- [15] HE Y J, LI Q L, LIU W. Effect of combined magnetic field on the eliminating inclusions from liquid aluminum alloy [J]. *Materials Letters*, 2011, 65(8): 1226–1228.

## 5083 铝镁合金熔炼净化工艺和细化效果

马成国, 亓淑艳, 李双, 胥焕岩, 何秀兰

哈尔滨理工大学 材料学院, 哈尔滨 150040

**摘要:** 高镁铝合金大规格铸锭的铸造工艺不够稳定, 从而影响最终产品质量。研究精炼、晶粒细化剂对 5083 铝合金组织和表面质量的影响。结果表明: 5083 合金旋转喷吹除气的优化精炼工艺为: 转速 250~400 r/min, 气体流量 1.2~2.0 L/s, 精炼时间 10~15 min。采用该优化的精炼工艺可使固体合金中气体含量降低至  $2 \times 10^{-3}$  mL/g 以下。晶粒细化剂的加入可以使 5083 合金的铸态组织细化。在加入的所有细化剂中, Al–5Ti–1B 丝具有最好的细化效果。随着细化剂加入量的增加, 细化效果提高。当 Ti 含量大于 0.1%, 细化效果变化不大。与使用其它细化剂的合金相比, 使用 Al–5Ti–1B 丝细化的合金表面很容易产生褶皱缺陷。

**关键词:** 铝镁合金; 熔炼; 净化工艺; 晶粒细化剂

(Edited by Chao WANG)